Adaptation of the residual vector for unknown dynamics
Physical Human Robot Interaction

Valentina Piccione 2030930

September 3, 2024

Abstract

In this study, the challenge of collision detection is addressed, being a crucial aspect in ensuring safe physical interactions between humans and robots. In particular a momentum-based residual with adaptive update strategy of dynamic parameters is developed for the robot collision detection. The proposed method integrates the dynamic model of a robotic system with real-time estimation of dynamic parameters. A regressor matrix is used to estimate and update the dynamic parameters adaptively, allowing the system to detect to external disturbances. The effectiveness of this approach is demonstrated through simulation, where the robot's trajectory, dynamic responses, and the evolution of the momentum residual are analyzed under varying conditions.

1   Introduction

Over the past few decades, the role of robots in industrial production and human services has evolved significantly. Initially confined to operating on factory floors and isolated from human interaction, with the advent of Industry 4.0 and smart manufacturing has spurred a growing demand for collaborative robots, or cobots, which share workspaces with humans.

Cobots are in fact designed to work alongside human operators in dynamic and unstructured environments. With this shift towards human-robot collaboration, it is critical to ensure safety during physical interactions.

A particular note of attention is to be placed on the detection, management and rapid response of accidental collisions between humans and robots.

Two primary approaches have been developed to address *collision detection*: sensor-based and model-based methods. Sensor-based methods leverage external sensors, such as cameras and force/torque sensors, which are utilized to monitor the robot's environment and detect collisions effectively, but with heavy costs and complexity to integrate into existing systems. In contrast, model-based methods rely on the robot's internal signals and dynamic models to detect collisions.

Still model-based methods are highly dependent on accurate dynamic parameters, which can vary due to factors such as joint friction, wear, and environmental changes. In this work these challenges are addressed by *adaptive strategy*: the momentum residual under the contact free situation can be adjusted adaptively according to the defined adaptive rate and the dynamic parameters of the robot can be continuously estimated, updated and refined during the working time of the robot instead of using default values given by dynamic identification.

2 Dynamic parameters

Considering a generic robot manipulator with n rigid joints arranged in an open kinematic chain, the canonical dynamical model is usually described as the Lagrange form

$$\boldsymbol{M}(\boldsymbol{q})\ddot{\boldsymbol{q}} + \boldsymbol{C}(\boldsymbol{q},\dot{\boldsymbol{q}})\dot{\boldsymbol{q}} + \boldsymbol{G}(\boldsymbol{q}) + \boldsymbol{\tau}_f = \boldsymbol{\tau} + \boldsymbol{\tau}_{ext} \tag{2.1}$$

where $\boldsymbol{q}, \dot{\boldsymbol{q}}, \ddot{\boldsymbol{q}} \in \mathbb{R}^{n \times 1}$ are the joint positions, velocities and accelerations, $\boldsymbol{M}(\boldsymbol{q}) \in \mathbb{R}^{n \times n}$ is the symmetric and positive definite inertia matrix, $\boldsymbol{C}(\boldsymbol{q}, \dot{\boldsymbol{q}}) \in \mathbb{R}^{n \times 1}$ is the Coriolis and centrifugal forces vector, $\boldsymbol{G}(\boldsymbol{q}) \in \mathbb{R}^{n \times 1}$ is the gravity vector and $\boldsymbol{\tau}_f$ is the friction torques inside the joints.
On the right side of the equation $\boldsymbol{\tau}$ represents the torques exerted by the joins and $\boldsymbol{\tau}_{ext}$ is the external torques generated by the collision of the robot with the surrounding environment.

The friction torque $\boldsymbol{\tau}_f$ has been computed following the equation

$$\boldsymbol{\tau}_f = \boldsymbol{f}_v \dot{\boldsymbol{q}} \tag{2.2}$$

where $\boldsymbol{f}_v \in \mathbb{R}^{n \times 1}$ is the vector of the viscous friction parameters arbitrarily chosen.

When $\boldsymbol{\tau_{ext}} = 0$ the manipulator is considered to move in a free space and its dynamic characteristics from the equation in 2.1 can be rearranged as a linear combination of the inertial parameters

$$\boldsymbol{\tau} = \boldsymbol{Y}(\boldsymbol{q}, \dot{\boldsymbol{q}}, \ddot{\boldsymbol{q}})\boldsymbol{X} \tag{2.3}$$

with $\boldsymbol{Y}(\boldsymbol{q}, \dot{\boldsymbol{q}}, \ddot{\boldsymbol{q}}) \in \mathbb{R}^{n \times c}$ the regressor matrix, and $\boldsymbol{X} \in \mathbb{R}^c$ the vector of inertial parameters. The latter comprises all the dynamic coefficients of the manipulator such as masses, moments of inertia, and the first moments (related to the center of mass) of the links in the manipulator.

The external torque $\boldsymbol{\tau_{ext}}$ has been modeled considering $\boldsymbol{\mathcal{F}}_{ext} \in \mathbb{R}^n$ the collision force applied on the end-effector of the manipulator $\boldsymbol{p_e} \in \mathbb{R}^n$, and the Jacobian of the manipulator $\boldsymbol{J_e}(\boldsymbol{q}) \in \mathbb{R}^{n \times n}$ associated to the collision point. The torque $\boldsymbol{\tau_{ext}}$ is then given by the equation

$$\boldsymbol{\tau_{ext}} = \boldsymbol{J}(\boldsymbol{q})^T \boldsymbol{\mathcal{F}}_{ext} \tag{2.4}$$

3 Adaptive parameters update

In the collision detection phase is crucial to assess whether a physical collision has occurred. On this matter a strategy for updating dynamic parameters is introduced to adapt to changing conditions and maintain momentum residuals within a stable range.

Firstly is important to define the generalized momentum of the robot $\boldsymbol{p}$. To do so the factorization of the Coriolis and centrifugal term is used, and so the property of skew-symmetry of the mass matrix $\dot{\boldsymbol{M}}(\boldsymbol{q}) - 2\boldsymbol{C}(\boldsymbol{q}, \dot{\boldsymbol{q}})\dot{\boldsymbol{q}}$ can be rewritten as

$$\dot{\boldsymbol{M}}(\boldsymbol{q}) = \boldsymbol{C}^T(\boldsymbol{q}, \dot{\boldsymbol{q}}) + \boldsymbol{C}(\boldsymbol{q}, \dot{\boldsymbol{q}}) \tag{3.1}$$

Thus the generalized momentum of the robot can be defined as

$$\boldsymbol{p} = \boldsymbol{M}(\boldsymbol{q})\dot{\boldsymbol{q}} \tag{3.2}$$

and given 2.1 and 3.1 its time evolution is

$$\dot{\boldsymbol{p}} = \boldsymbol{C}(\boldsymbol{q}, \dot{\boldsymbol{q}})^T\dot{\boldsymbol{q}} - \boldsymbol{G}(\boldsymbol{q}) - \boldsymbol{\tau}_f + \boldsymbol{\tau} + \boldsymbol{\tau}_{ext} \tag{3.3}$$

Additionally also the time evolution of the estimation of the generalized momentum can be defined as

$$\dot{\hat{\boldsymbol{p}}} = \hat{\boldsymbol{C}}(\boldsymbol{q}, \dot{\boldsymbol{q}})^T\dot{\boldsymbol{q}} - \hat{\boldsymbol{G}}(\boldsymbol{q}) - \boldsymbol{\tau}_f + \boldsymbol{\tau} + \boldsymbol{r} \tag{3.4}$$

A key component of the collision detection is the computation of the momentum residual. It represents the difference between the expected momentum, based on the robot's dynamic model, and the actual momentum observed during operation. Operating under normal conditions without any external interference, the momentum residual of the manipulator should be close to zero. However, if an unexpected force or collision occurs, the residual will deviate, indicating a discrepancy between the expected and actual behavior of the robot.

Based on 3.3 and 3.4 the dynamics of the momentum residual can be computed as

$$\dot{\boldsymbol{r}} = \boldsymbol{K}(\dot{\boldsymbol{p}} - \dot{\hat{\boldsymbol{p}}}) \tag{3.5}$$

where $\boldsymbol{K}$ is a diagonal gain matrix for the Momentum Residual constituted as

$$\boldsymbol{K} = \boldsymbol{k}\boldsymbol{I}_{3x3} \tag{3.6}$$

The estimation of the momentum residual is then retrieved by integration of 3.5

$$\hat{\boldsymbol{r}} = \boldsymbol{K} \int_0^t (\boldsymbol{\tau}_{ext} - \hat{\boldsymbol{r}})dt \tag{3.7}$$

that considering $\boldsymbol{\tau}_{ext} = \boldsymbol{\tau} - \boldsymbol{Y}(\boldsymbol{q}, \dot{\boldsymbol{q}}, \ddot{\boldsymbol{q}})\boldsymbol{X}$ can be rearranged as

$$\hat{\boldsymbol{r}} = \boldsymbol{K} \int_0^t (\boldsymbol{\tau} - \boldsymbol{Y}(\boldsymbol{q}, \dot{\boldsymbol{q}}, \ddot{\boldsymbol{q}})\boldsymbol{X} - \hat{\boldsymbol{r}})dt \tag{3.8}$$

It can be noticed that 3.8 depends on the vector of dynamic parameters $\boldsymbol{X}$. Whenever these parameters are inaccurate, or change it results in an increased momentum residual,

3

which can compromise the accuracy of collision detection.

Conversely, because momentum residuals are highly sensitive to dynamic parameters, the residuals observed when no collision occurs can serve as an indicator of the accuracy of dynamic identification and whether the parameters have shifted during the robot's operation.

If high residuals are detected even in the absence of a collision, it suggests that the dynamic parameter identification is currently inaccurate.
In cases where a robot is used continuously, a consistently rising momentum residual typically signals that the dynamic parameters have altered.
Therefore, the adaptive adjustment of the robot's dynamic parameters based on the momentum residuals observed at each joint when no collision is occurring is crucial.

The adaptive rate of the dynamics parameters can then be defined as

$$\begin{cases} \dot{\hat{X}} = \boldsymbol{\lambda}_1^{-1} \boldsymbol{Y}^T(\boldsymbol{q}, \dot{\boldsymbol{q}}, \ddot{\boldsymbol{q}}) \hat{\boldsymbol{r}} + \boldsymbol{\lambda}_2^{-1} \boldsymbol{Y}^T(\boldsymbol{q}, \dot{\boldsymbol{q}}, \ddot{\boldsymbol{q}}) \dot{\boldsymbol{r}} \\ \hat{\boldsymbol{X}}(t) = \hat{\boldsymbol{X}}(t-1) + \dot{\hat{\boldsymbol{X}}}(t) \cdot \Delta t \end{cases} \tag{3.9}$$

where $\boldsymbol{\lambda}_1$ and $\boldsymbol{\lambda}_2$ are two positive definite matrices and $\dot{\hat{X}}$ is the rate of change of the dynamic parameters. The two matrices $\boldsymbol{\lambda}_1$ and $\boldsymbol{\lambda}_2$ represents weighting factors controlling the contribution of the respective terms to the overall output.

4 Experimental part

4.1 Robot parameters

The robot being considered is a spatial 3R elbow-type manipulator, with each link treated as a uniform cylinder. It is assumed that each link of the robot is a rigid body with uniform mass distribution and the center of mass for each link is located halfway along its axis. The dynamic parameters and the Denavit-Haremberg parameters are reported in the Tables 1 and 2:

	joint 1	joint 2	joint 3
α	$\pi/2$	0	0
a	0	0.5	0.4
d	0.5	0	0
θ	q_1	q_2	q_3

Table 1: DH table

	Mass [kg]	Radius [m]
link 1	15	0.2
link 2	10	0.1
link 3	5	0.1

Table 2: Dynamic parameters

4

4.2 Trajectory

A desired motion for the end-effector is defined by $\boldsymbol{p}_{e,d}$, $\dot{\boldsymbol{p}}_{e,d}$, $\ddot{\boldsymbol{p}}_{e,d}$, with $\boldsymbol{p}_{e,d} \in \mathbb{R}^3$ end-effector position, and then translated into the joint space $\boldsymbol{q}_d$, $\dot{\boldsymbol{q}}_d$, $\ddot{\boldsymbol{q}}_d$.

This trajectory is intended to excite the robot's joints by moving its end-effector through a specific path, which is shaped like an ellipsoid in 3D space.

The profile of the desired end-effector quantities is reported in Figure 1.
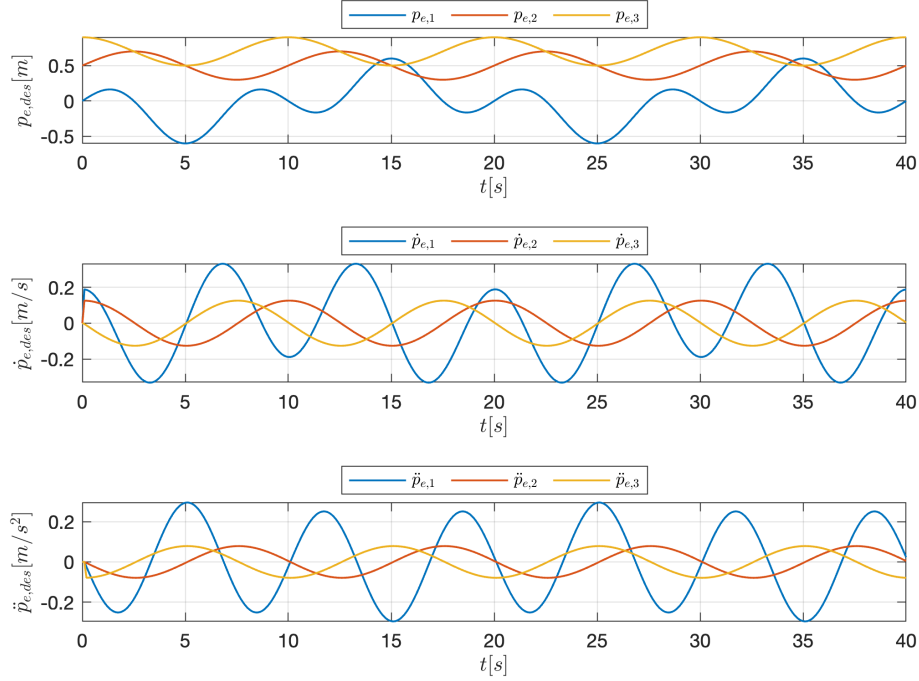
Figure 1: The desired end-effector position (top), velocity (middle) and acceleration (bottom).

4.3 External torque generation

In order to simulate human collision with the manipulator, external forces are applied at the end-effector at certain time intervals during its motion. The generated force profile $\boldsymbol{\mathcal{F}}_{ext} = (\boldsymbol{f}_{ext}^x, \boldsymbol{f}_{ext}^y, \boldsymbol{f}_{ext}^z)^T$ is used in 2.4 to compute $\boldsymbol{\tau}_{ext}$ and feed it in input to the manipulator. Both the external force and torque profile can be seen in Figure 2.

The force profile is constituted as follows: the first push is a vector $\boldsymbol{\mathcal{F}}_{ext} = [-25, 5, 0]^T$ at simulation time $4s$ with a duration of $1s$, pushing the robot end-effector towards the outside of the desired trajectory. The second push is a shorter and less intense impulse represented by a vector $\boldsymbol{\mathcal{F}}_{ext} = [0, -15, 5]^T$ at simulation time $33s$ with a duration of $0.35s$.
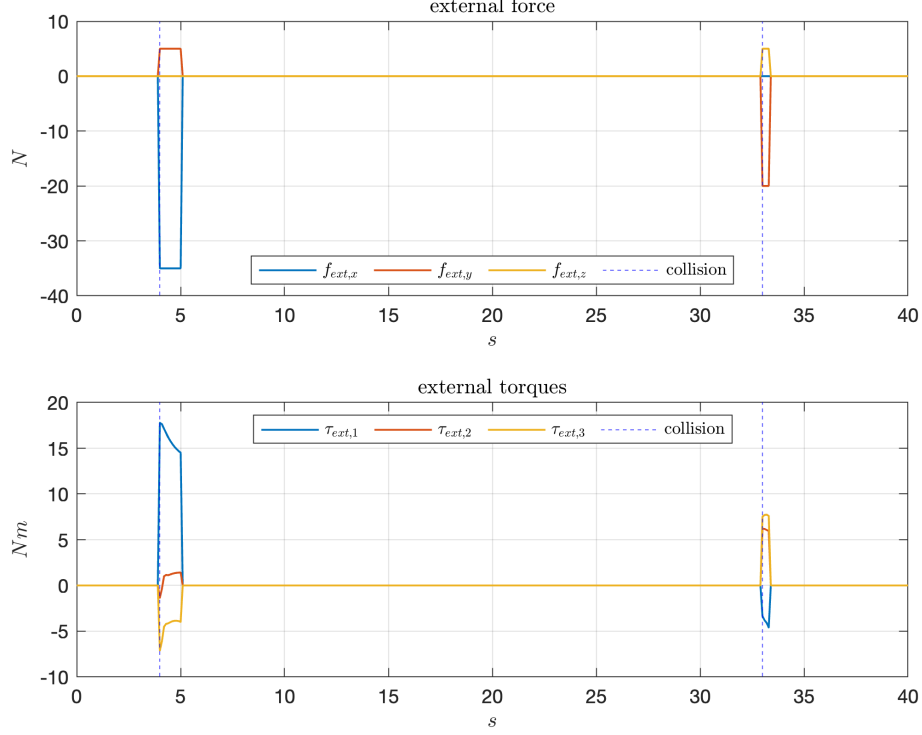
Figure 2: The external force applied at the end effector (top) and the resulting torque (bottom).

4.4 Controller

Given the desired joint trajectories velocities and accelerations $(\boldsymbol{q}_d, \dot{\boldsymbol{q}}_d, \ddot{\boldsymbol{q}}_d)$ from the trajectory generation and the partially estimated state of the robot $(\hat{\boldsymbol{q}}, \dot{\hat{\boldsymbol{q}}})$, a control strategy based on Feedback Linearization is implemented as follows

$$\boldsymbol{\tau} = \hat{\boldsymbol{M}}(\hat{\boldsymbol{q}})[\ddot{\boldsymbol{q}}_d + \boldsymbol{K}_p(\boldsymbol{q}_d - \hat{\boldsymbol{q}}) + \boldsymbol{K}_d(\dot{\boldsymbol{q}}_d - \dot{\hat{\boldsymbol{q}}})] + \hat{\boldsymbol{C}}(\hat{\boldsymbol{q}}, \dot{\hat{\boldsymbol{q}}})\dot{\hat{\boldsymbol{q}}} + \hat{\boldsymbol{G}}(\hat{\boldsymbol{q}}) + \boldsymbol{\tau}_f \qquad (4.1)$$

where $\boldsymbol{K}_p, \boldsymbol{K}_d$ diagonal gain matrices constituted as

$$\boldsymbol{K}_d = \boldsymbol{k}_d \boldsymbol{I}_{3x3} \qquad \text{and} \qquad \boldsymbol{K}_p = \boldsymbol{k}_p \boldsymbol{I}_{3x3} \qquad (4.2)$$

with the following properties: $\boldsymbol{k}_p, \boldsymbol{k}_d > 0$ to maintain stability, $\boldsymbol{k}_d = 2\sqrt{\boldsymbol{k}_p}$ to have critically damped response.

This scheme integrates feedforward control with a proportional-derivative (PD) controller to achieve accurate tracking of the desired motion.
Ideally $\hat{\boldsymbol{M}}(\hat{\boldsymbol{q}}) = \boldsymbol{M}(\boldsymbol{q})$, $\hat{\boldsymbol{C}}(\hat{\boldsymbol{q}}, \dot{\hat{\boldsymbol{q}}}) = \boldsymbol{C}(\boldsymbol{q}, \dot{\boldsymbol{q}})$, $\hat{\boldsymbol{G}}(\hat{\boldsymbol{q}}) = \boldsymbol{G}(\boldsymbol{q})$, $\hat{\boldsymbol{q}} = \boldsymbol{q}$ and $\dot{\hat{\boldsymbol{q}}} = \dot{\boldsymbol{q}}$ and a linear and decoupled behaviour is achieved.

4.5 Simulation

The experiment is validated via a $40s$ simulation in which the end-effector is located in position $\boldsymbol{p}_e = [0, 0.5, 0.9]^T$, with a joint configuration $\boldsymbol{q} = [\pi/2, 0, \pi/2]^T$ and initial velocity and acceleration $\dot{\boldsymbol{q}}, \ddot{\boldsymbol{q}} = 0$.
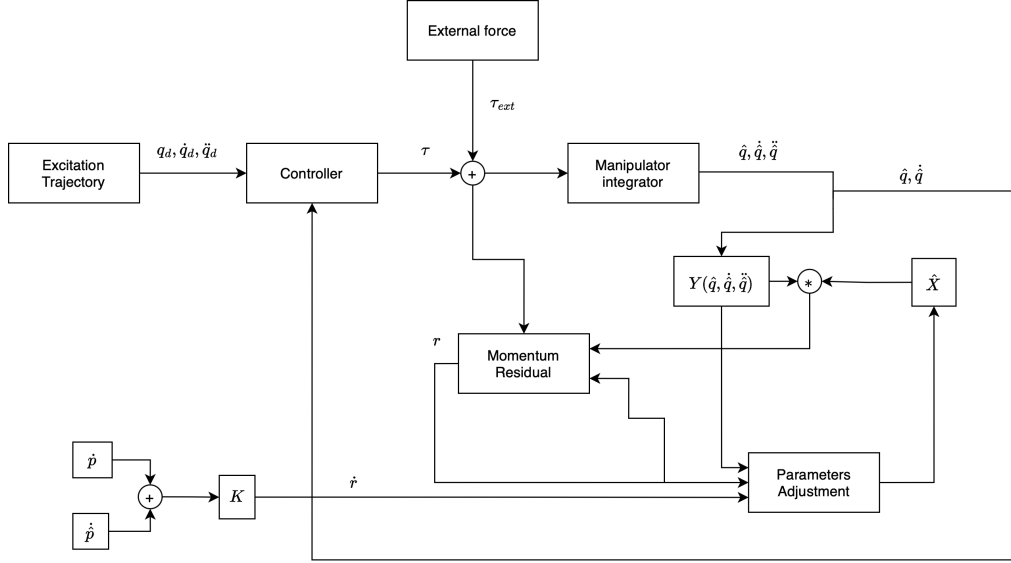The procedure is presented in the block scheme in Figure 3.

Figure 3: Block scheme of the simulation loop.

The robot starts moving following the previously specified excitation trajectory, in which all the joints are moving. From the joint position $\boldsymbol{q}$ and the end-effector velocity and acceleration $\dot{\boldsymbol{p}}_e, \ddot{\boldsymbol{p}}_e$, the velocity $\dot{\boldsymbol{q}}$ and acceleration $\ddot{\boldsymbol{q}}$ are obtained by inverse differential kinematics, and thereafter used to compute the torque $\boldsymbol{\tau}$ using the formula 4.1. The computed variables, $\boldsymbol{\tau}, \boldsymbol{q}, \dot{\boldsymbol{q}}, \ddot{\boldsymbol{q}}$ are the input parameters of the overall algorithm for updating the dynamic parameters $\boldsymbol{X}_i$.

The matrix $\boldsymbol{Y}$ is computed with the values of $\boldsymbol{q}, \dot{\boldsymbol{q}}, \ddot{\boldsymbol{q}}$ of the current step, and the values of the evolution of the generalized momentum and of its estimation, $\dot{\boldsymbol{p}}$ and $\dot{\hat{\boldsymbol{p}}}$ are computed respectively as in 3.3 and 3.4 again with the current step values.
The newly estimated quantities are necessary for the computation of the momentum residual $\boldsymbol{r}$, that is then obtained through 3.8, and of its dynamics $\dot{\boldsymbol{r}}$ obtained through 3.5.

Then, according to the equation 3.9, the obtained residuals and previously determined motion data $\boldsymbol{q}, \dot{\boldsymbol{q}}, \ddot{\boldsymbol{q}}$ are used to update the parameters of the last step. Finally the updated parameters $\hat{\boldsymbol{X}}(\boldsymbol{t})$ are used in the computation of the momentum residual of the next step.

5   Results

For the implementation of the previously explained simulation the following values were chosen experimentally:

- the controller gains k_p and k_d set respectively to 80 and 15

- the residual gain k set as 0.2

- the lambda matrices parameters λ_1 and λ_2 set respectively to 1.5 and 1.1. These values were chosen so as for the system to quickly adjust based on the inputs.

- the viscous friction values set to 2

- the upper and lower threshold values of the momentum residual set respectively to 2 and -1.4

5.1   Contact-free

Firstly a simulation in a contact-free environment is performed, in order to evaluate the results of the controller, the residual computation and compare the results with the simulation where collisions are present.

The controller results are evaluated and showed in Figures 4a, 4b, 5a and 5b.
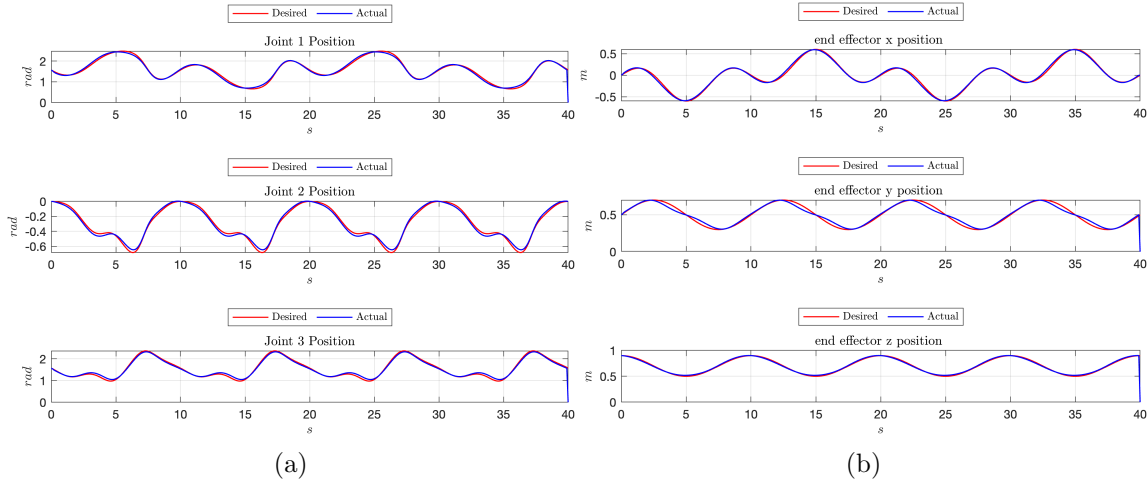
Figure 4: The joints position (a) and the end-effector position (b) in the collision-free simulation.

It can be noticed that the actual joints position follow closely the desired ones, and the position of the end-effector follows the desired course, without particular deviations, while the actual velocity and the acceleration follow the desired profile but with some small deviations, due to inaccuracies of the controller utilized in the simulation.
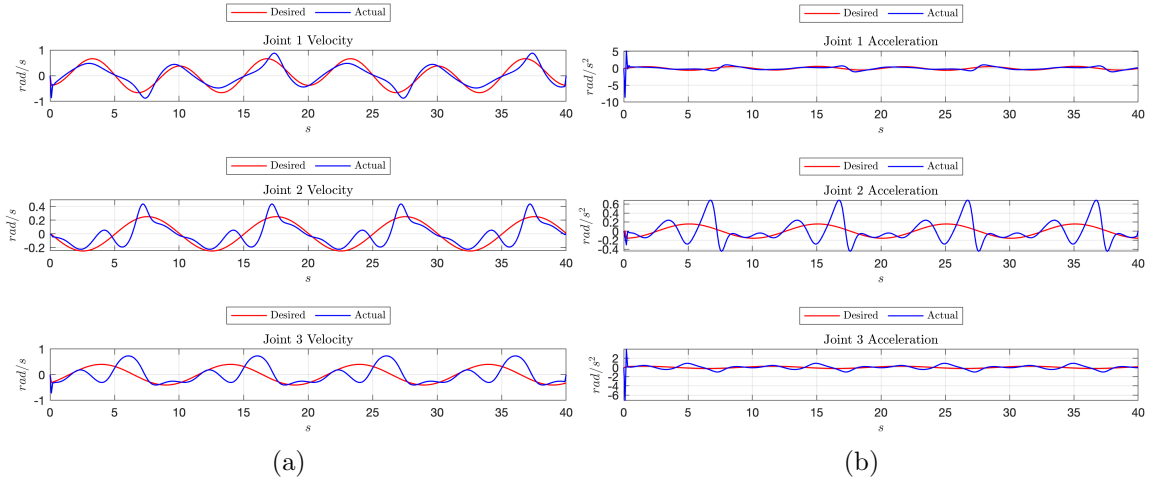
Figure 5: The joints velocity (a) and acceleration (b) in the collision-free simulation.

The update of the dynamic parameters in the collision-free environment is reported in Figure 6, showing a stable evolution of all the elements of the $\boldsymbol{X}$ vector.

Figure 7 represents the momentum residual of the contact-free simulation. It can be noticed that however oscillating, the values of the residual of all the joints remains in the
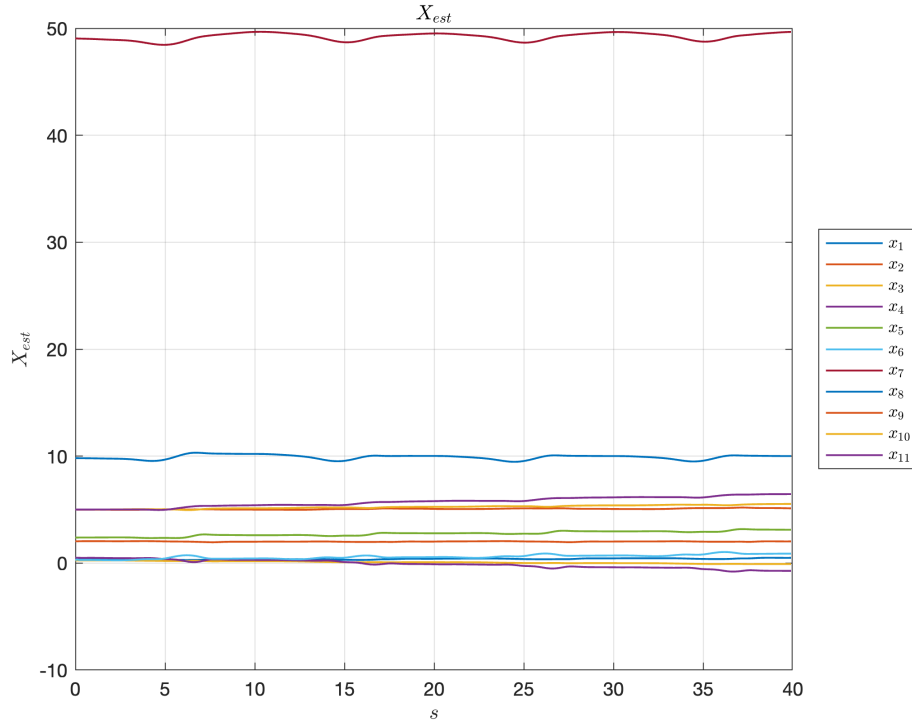

Figure 6: Dynamic parameters update in a contact-free simulation.

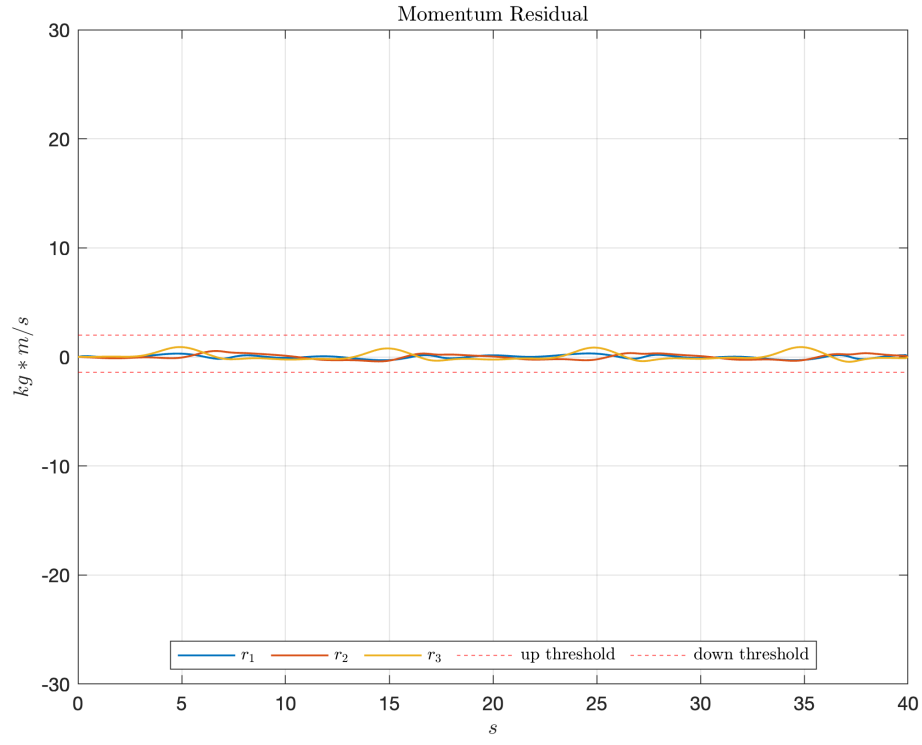range of 0 as expected, and never exceed the designed thresholds.

Figure 7: The evolution of the momentum residual during the simulation in a contact-free space.

5.2 Collision test

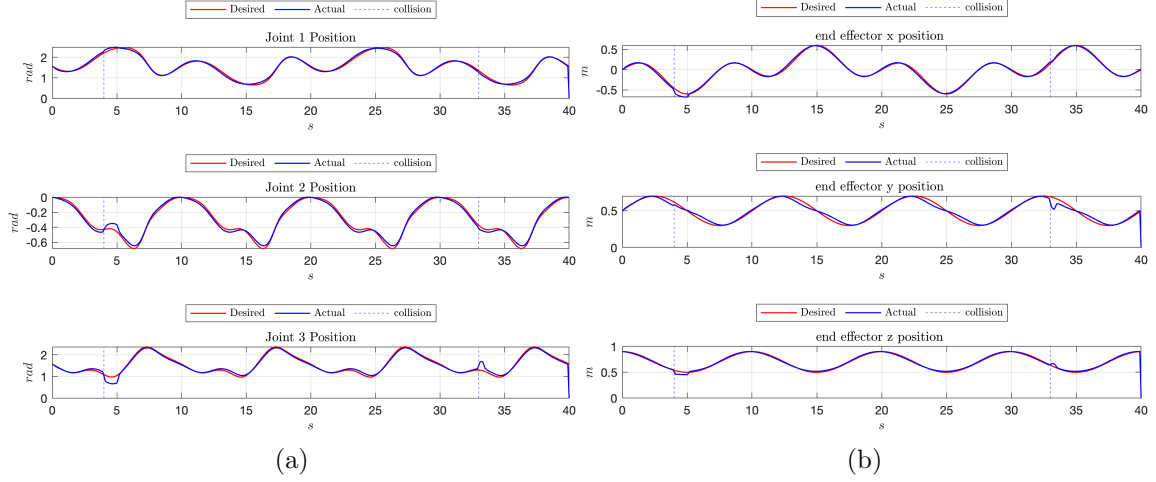Subsequently the two collisions are introduced in the simulation.

(a)   (b)

Figure 8: The joints position (a) and the end-effector position (b) in the collision simulation.

As for the previous simulation the joints and the end-effector actual position, represented in Figures 8a and 8b, follow closely the desired profile, except for the points where collisions occur.

In particular regarding the joints position in the first collision both joints 2 and 3 have a sharp deviation, while in the second collision the deviation is clearer only on joint 3, because of how this collision is modeled.

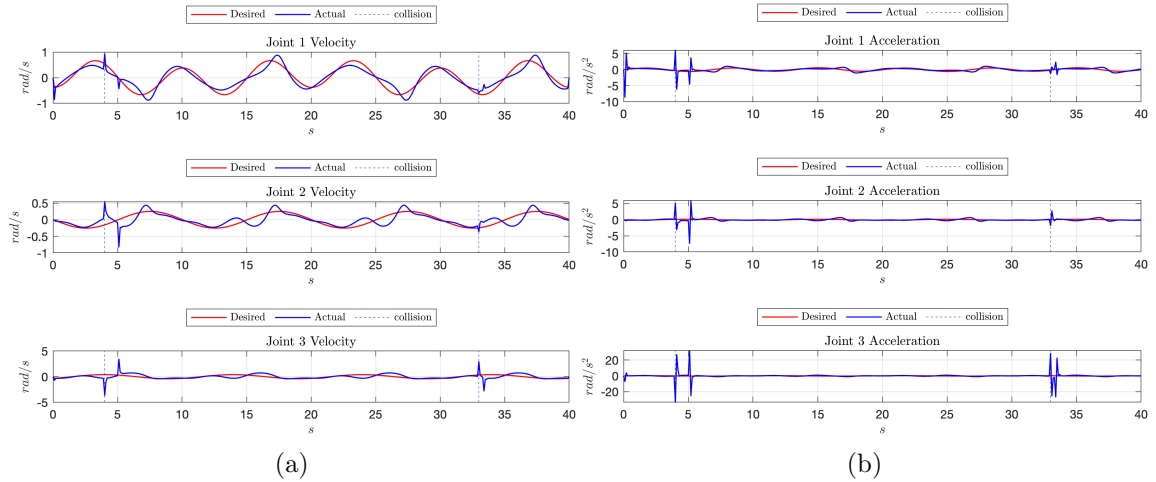(a)   (b)

Figure 9: The joints velocity (a) and acceleration (b) in the collision simulation.

This sudden movement of the joints is reflected also in the end-effector position that de-

11

viates from the path at collision time. In fact for the first collision the deviation of the actual end-effector position is visible on the x and y axes, while on the second collision is visible on the y and z axes.

Uncertainties present in the velocity and acceleration of the joints are visible in Figures 9a and 9b, at all times, including at the collisions where there are small peaks in both velocity and acceleration for all the joints, due to the occurrence of the impacts.
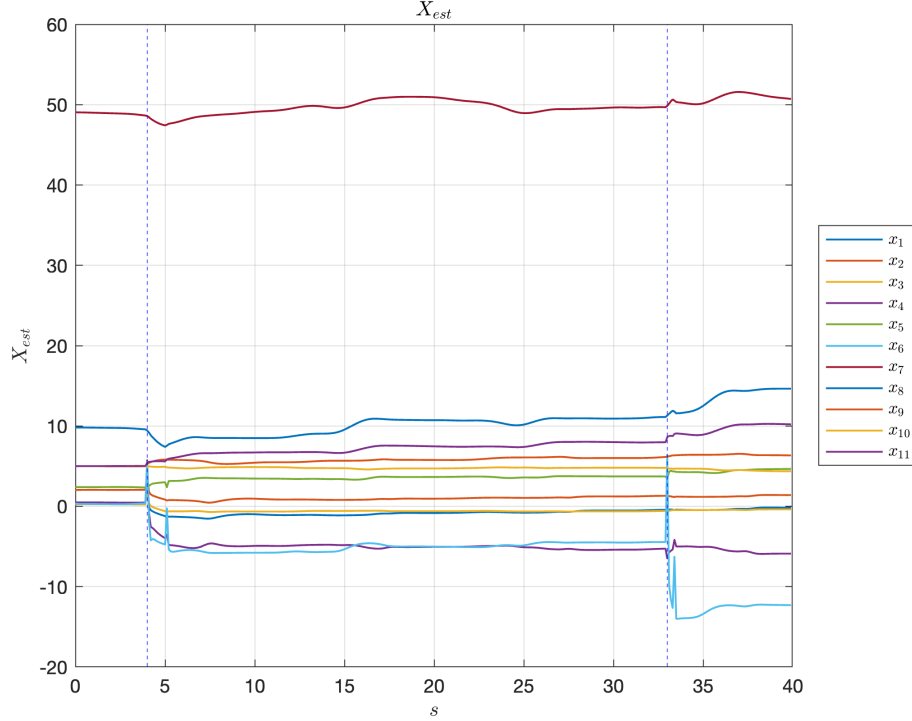

Figure 10: Dynamic parameters update during the collision simulation. The elements x_4 and x_6 are represented respectively by the violet and cyan lines further down in the graph.

Figure 10 and 11 report respectively the dynamic parameters update and the momentum residual of the collision simulation.
It can be noticed that the $\boldsymbol{X}$ vector presents more oscillations than the previous simulation, both collisions are particularly visible and the most affected elements are x_4 and x_6 that presents spikes at the collision times and clear variations of their value after the collisions occurred.

The momentum residual $\boldsymbol{r}$ in the first part of the simulation before the first collision is stable and very close to the 0 value for all the joints as for the previous simulation.
At $t = 4s$ the first collision occurs and the residual of the joints instantaneously increase. The residual of all three joints have a clear peak, but only the residual of joint 3 exceed the designed threshold detecting a collision with a peak of $-4.61\ kg \cdot m/s$.
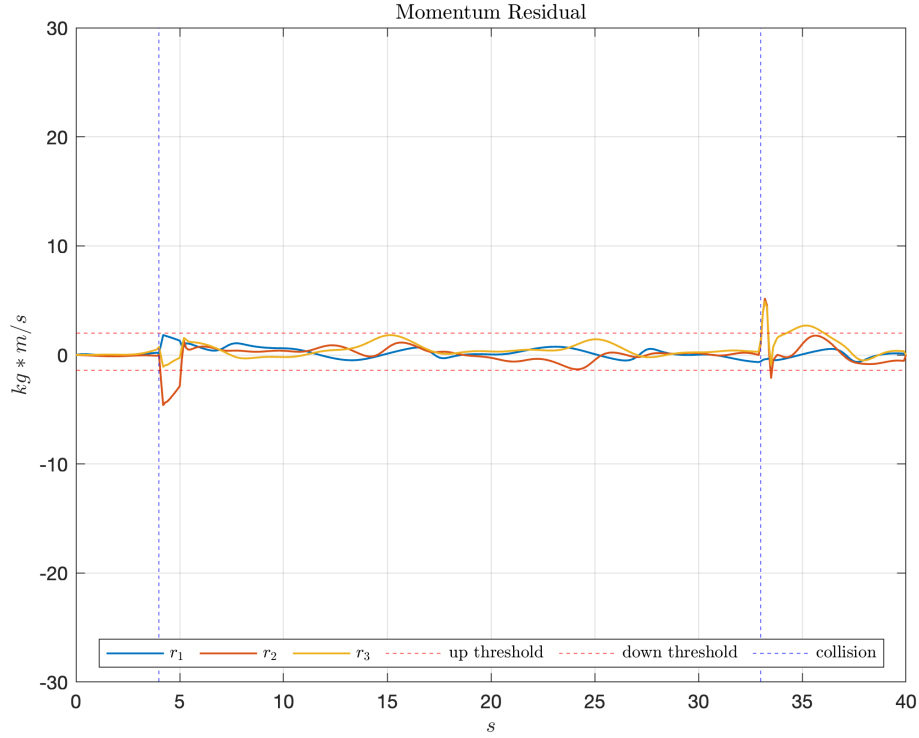
Figure 11: The evolution of the momentum residual during the collision simulation.

After the first collision the robot continues moving in a collision-free space and the residual of the three joints, even with some small variations, settles back without exceeding the threshold.

At $t = 33s$ the second collision occurs and again the momentum residual of the joints 2 and 3 increase instantaneously. In this case the collision is a shorter impact, but generates higher values in the residual, with peaks of respectively $5.15\ kg \cdot m/s$ and $4.9\ kg \cdot m/s$ and with a major difficulty in set back again in the around of 0.

6   Conclusions

In this work, the performance of an adaptive momentum-based residual strategy for collision detection in robotic systems has been successfully demonstrated.
By continuously updating dynamic parameters during operation, the method enhances the accuracy of collision detection, particularly in scenarios where dynamic parameters may vary due to factors such as joint friction or environmental changes.

The proposed approach was validated through simulations including both contact-free scenarios and controlled collision tests.
In the contact-free simulation the dynamic parameters showed stable evolution, and the

momentum residuals remained close to zero, confirming the system's ability to maintain accurate dynamic parameter identification in the absence of external disturbances.

During the collision tests, the system effectively detected external forces applied at specific intervals, showing the capacity to detect and respond to collisions, underscoring the effectiveness of the adaptive momentum residual approach.